Timescales and Phenomenology of Mechanically Stimulated Glasses: a Review

Alberto D'Amore,[1] *Luigi Grassia,**[1] *Domenico Acierno*[2]

Summary: The principal features of the volumetric as well as the viscoelastic response of mechanically stimulated glasses can be summarized as follows: i) the time-aging time shift factors contract upon increasing the probe stress (i.e. the stress apparently modifies the volume recovery kinetics), ii) the volume recovery baseline remains unaltered (i.e. the underlying structure of the stimulated glass remains unchanged) iii) yielding scales linearly with the logarithmic of the strain rate. Here we present a review of the above features with aid of a series of numerically simulated results concerning the responses of glassy polycarbonate. Simulations are obtained coupling a modified KAHR equation with the constitutive law for linear viscoelasticity within the domain of the reduced time. It will be shown that by using a minimum of experimental (PVT and linear viscoelastic) data inputs even the subtle intricacies can be predicted. Furthermore a new class of results concerning the stress-strain behaviour of glassy polymers is presented that never appeared before.

Keywords: glass transition; structure-property relations; viscoelastic properties; yielding

Introduction

In the last three decades a huge number of experimental results have been presented concerning the effects of mechanical loadings on the thermodynamic state of amorphous glassy materials.[1,2] Whether the mechanical stress alters the glassy "structure" or not was the source of excited debates.

"*If the mechanical perturbation alters the underlying structure of the glass, this must be accounted for explicitly in any constitutive law description of the behaviour. On the contrary, the mechanical response is a function only of the current state of the glass and one is not required to consider explicitly any alterations in the glassy structure due to the mechanical perturbations*".[2] Thus, solving the problem involves primarily defining its level of complexity. Looking at the actual scenario one can easily realize that, from one side, the structural relaxation of unperturbed glasses can be reliably described by phenomenological[3,4] as well as pseudo-thermodynamic theories,[5] so that one can predict with accuracy the PVT curves of any glass forming material subjected to arbitrary thermal and/or pressure histories. On the other hand. "*when materials with finite dimensions subjected to any loading and/or thermal history are of concern, none of the available theories of the glassy state contain the essential ingredients to follow the kinetics of structural relaxation at each body point*".[6] In this paper we restrict the discussion to polymer glasses and describe a series of inherent difficulties arising from the study of mechanically stimulated glasses. The reason lies primarily in the fact that the phenomenological intricacy can only be clarified starting from irrefutable premises. Missing such premises has led some authors to completely divergent conclusions even in presence of the same experimental

---

[1] The Second University of Naples-SUN, Dipartimento di Ingegneria Aerospaziale e Meccanica Via Roma 19, 81031 Aversa (CE) Italy
E-mail: luigi.grassia@unina2.it

[2] University of Naples Federico II, Department of Materials and Production Engineering, P.le Tecchio 80125 Naples, Italy

evidences.[2,7] Then, a series of numerically obtained data (to be considered as replicas of the relevant experimental results appeared in literature) will provide some insights concerning the origin of the time-scales modifications of both volumetric and viscoelastic responses. Finally, the stress-strain behaviour of glasses will be depicted with aid of a brand new set of simulation.

Phenomenological and Theoretical Intricacy

The experimental difficulties arising from the study of mechanically stimulated glasses are outlined in what follows:

a) glasses are rheologically complex materials as their viscoelastic response is a function of the kinetics of a structural variable. For instance, the viscoelastic responses of a glass subjected to creep tests performed at the same level of loading and different elapsed times may differ dramatically. Therefore, mechanical (viscoelastic) tests "must" be realised according to well defined protocols with the objective to surmount the rheological complexity. In Figure 1 one such protocols[1] (referred to as "Protocol I" or Struik protocol) is reported. The protocol I starts from a well defined "state" of the glass (generally obtained by down-quenching from above T_g to the test temperature). It is postulated that, during the mechanical loading interval, t_i, the glass preserves the "iso-structural" conditions, conforming to the assumption that the ongoing (spontaneous) structural changes are negligible with respect to those visited before the start of loading. With this procedure the viscoelastic responses were conceived to be free of the "actual" structure dependence and the time, t_{ei}, elapsed before each test, was assumed as the "structural parameter".

b) the volumetric measurements on mechanically loaded samples present inherent technical difficulties. In fact, the simultaneous viscoelastic and volumetric relaxation behaviour have been reported only for thickset samples in torsion, in the framework of protocol I, at the National Institute of Standards and Technology-NIST.[2] However, a substantial point (indeed rarely mentioned) arise from the fact that, within samples of finite size, the thermal histories suffered at each body point can differ greatly.[6] So that, even if

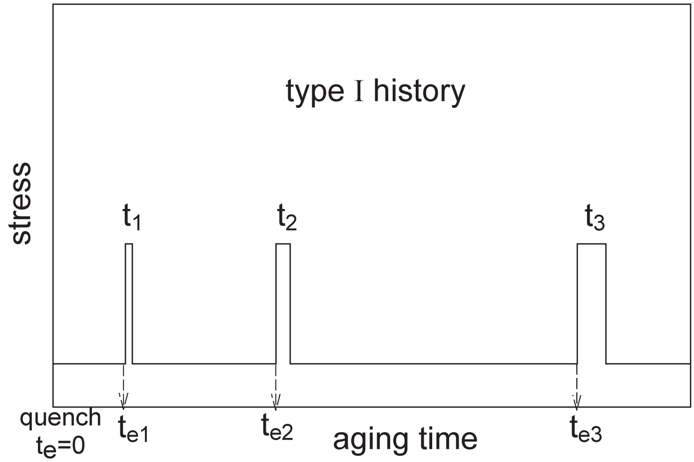

Figure 1.
Schematic of Protocol I. The symbols t_{ei} represent the aging times ($t_{ei} \approx 2t_{ei-1}$, i = 1,2.). The symbols t_i represent the loading times ($t_i/t_{ei} \leq 0.1$).

the isothermal conditions are achieved, the volumetric behaviour of the whole sample is the result of the different volume relaxation kinetics at each point. Furthermore, the mutual interactions arising from the differential volume variations of adjacent points give rise to adjunctive stresses (the residual stresses). This last aspect was recently resolved[8] and, fortunately, it can be accounted for theoretically. It was found[8] that, depending on the Biot number, freely standing (unloaded) samples with thickness in the range 5–10 mm (the size of samples used in practice) can exhibit residual stresses as high as 30 MPa (namely, more or less the half of the glassy polymers ultimate strength). Anyway, one can easily recognize that when glasses are mechanically loaded, the unavoidable presence of residual stresses compel inevitably a distortion of the local effective stresses along the sample thickness with respect to the nominal applied stress. For instance, even the simplest applied perturbation (namely, the loading conditions experienced under uniaxial tensile creep test) become rather complex while the experimental response (the creep compliance) requires deeper analysis.

c) Glassy polymers show a linear dependence of the yield stress on the logarithm of the deformation rate. This an important and intriguing point as the very existence of the yield stress (i.e. if it is a myth or an engineering reality), is still a matter of discussion.[9,10] To illustrate, at low strain rates the yield stress vanishes. Further, it will be shown in the following text that the ''aging time'' can play a dramatic role, a case rarely considered in literature.

From a theoretical viewpoint the state of the art can be outlined as follows:

a) There is a considerable body of literature that deals with the nonlinear viscoelasticity of glassy polymers that falls into the class of constitutive models that we refer to as ''material clock models''. Probably the best known model is the volume clock (or free volume clock) model of Knauss and Emri.[11] More recently, Lustig, Shay and Caruthers[12] and Caruthers, Adolf and Chambers[13,14] have carried out extensive analyses of a Rational Mechanics based nonlinear thermodynamics that they claim can do structural recovery and nonlinear viscoelasticity. Their approach is based on internal energy and appears of very general interest. However, the above mentioned theories do not address the phenomenology of mechanically stimulated glasses directly, at least in the light of the predictions of the substantial features discussed in the introduction that feed the debate along the years. So that, the capability of these models to predict of the main features of mechanically stimulated glasses remains unknown to the present authors. Very recently we have shown that[6] some features of mechanically stimulated glasses can be reliably predicted, under different loading protocols, even in their subtle characteristics.

b) Predicting the stress-strain behaviour of glassy materials is rather complicated. In fact, the material passes continuously from a glassy to a viscous-like behaviour at the yield point. Yielding was modelled by Eyring.[15] However, in the Eyring theory and the subsequent modifications none of the physical changes occurring before the yield point was accounted for. In fact, the process that involves a passage from a glassy to a liquid-like behaviour remained unexplained. Of course, explaining the physics underlying the passage from a glassy to a liquid-like (viscous) state during the stress-strain measurements would represent a formidable breakthrough in Materials Science. Here, again one can easily recognize that this class of problem can only be attacked with models that account for the simultaneous volumetric and viscoelastic behaviour.

Experimental Evidences and Numerical Simulations

Anyway, despite the phenomenological intricacy, the three substantial features of mechanically stimulated glasses that feed the debate along the years can be summarized as follows:

I) the mechanical stress reduces the glass stiffness (for instance, in a tensile creep test, the response in terms of creep compliance appears shifted towards left at higher stresses).[1] As a consequence, in the framework of the Protocol I, the time-aging time shift factors contract with the stress. From this behaviour one can argue that the stress alters the mechanical response or, in other words, the thermodynamic state of the glass (i.e. the timescales of the responses). The above occurrences are reflected in our simulations reported in Figure 2.

II) the "natural" volumetric relaxation (i.e. the relaxation that one observes in absence of mechanical loadings) represents the "baseline" to the "temporary" volumetric perturbations induced by mechanical loadings. This can be readily seen looking at Figure 3. Here the volumetric responses at different levels of stress are reported conforming to the loading protocol I. It is evident that, sooner or later (depending on the level of stress) upon unloading, the "latent" glassy state is recovered.[2] In addition one may observe that the simulation can capture some very subtle features reported in literature. For instance, we classify here some of them:

1. the small undershoots beneath the volume recovery baseline[2]
2. The "height" of the volumetric creep curves that increases with the aging time (this is not trivial: in ref.[6] it has been clarified that such behavior can be suitably used to explain the shift factors contraction)
3. The non-monotonic volume creep behavior at early stage of aging (this is also clearly apparent from a careful inspection of the volumetric data published by McKenna.[2] This is a dramatic probe of the interplay between stress and struc-

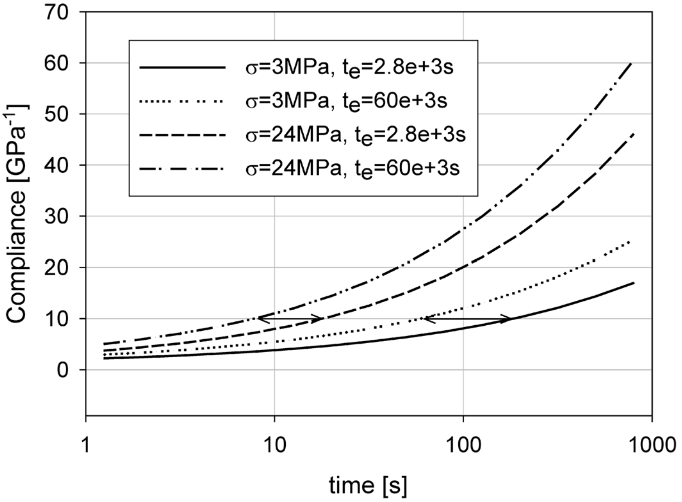

Figure 2.
Schematic of the impact of stress on the time-ageing time shift factors.

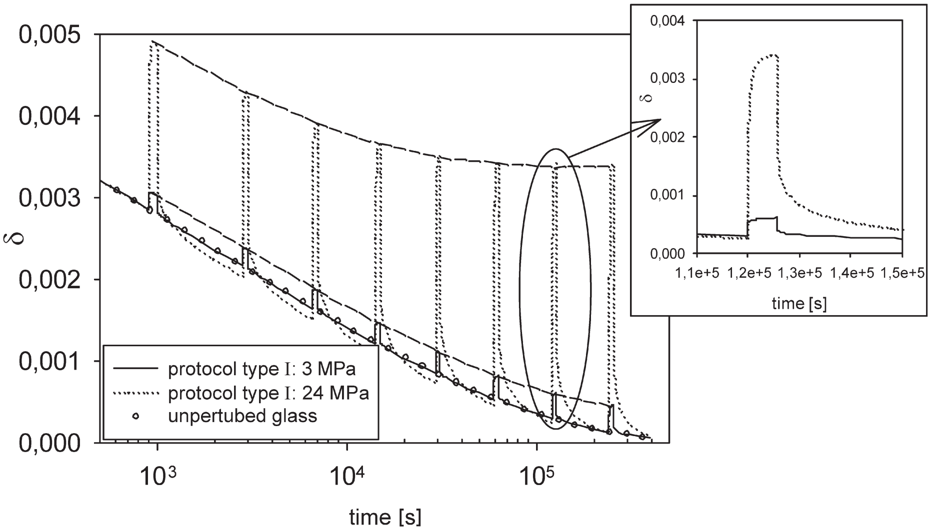

Figure 3.
Numerical simulation of the volumetric response within the protocol I. The insert shows the effect of stress on the volume recovery kinetics: the "baseline" is recovered "rapidly" at lower stresses. δ is the normalised distance from the equilibrium line.

ture even within the loading interval where, instead, the viscoelastic response was postulated free of a structural dependence (in the framework of protocol I).

III) yielding scales linearly with the logarithmic of the strain rate. In Figure 4a a typical "Eyring plot" is reported illustrating the above features. Simulations come again from our modelling approach that we recall for clarity purpose.

Theoretical Background

Our approach derives from the well established phenomenological theories capable of capturing the principal features (nonlinearity and memory effect) of structural relaxation. In this respect both KAHR (Kalroush, Aklonis, Hutchinson, Ramos)[3] and TNM (Tool-Narayanaswamy-Moynihan)[4] theories predict with accuracy the PVT curves of any glass forming material. Indeed, KAHR theory accounts explicitly for the (external) pressure and represents a more viable formalism for our purposes. However the available phenomenological theories of the glassy state do not contain the essential *ingredients* to follow the volume and/or enthalpy recovery kinetics in bodies of "finite" dimensions.

For instance, when dealing with dilatometric experiments on objects of finite size, one measures the overall volume variations (under given thermal histories) as a sum of the individual contributions of each body point. However, the individual points are subjected to different stimuli (caused by transient heat transfer phenomena) that give rise to different structural relaxation kinetics. At the same time arbitrary mechanical loadings would produce different volumetric effects on the individual body points. Locally, the time dependent volume variations due to the mechanical stress are debited to the isotropic part of the stress tensor through the "local" bulk relaxation modulus.

To better clarify, in Figure 5 the background of the phenomenology is illustrated:

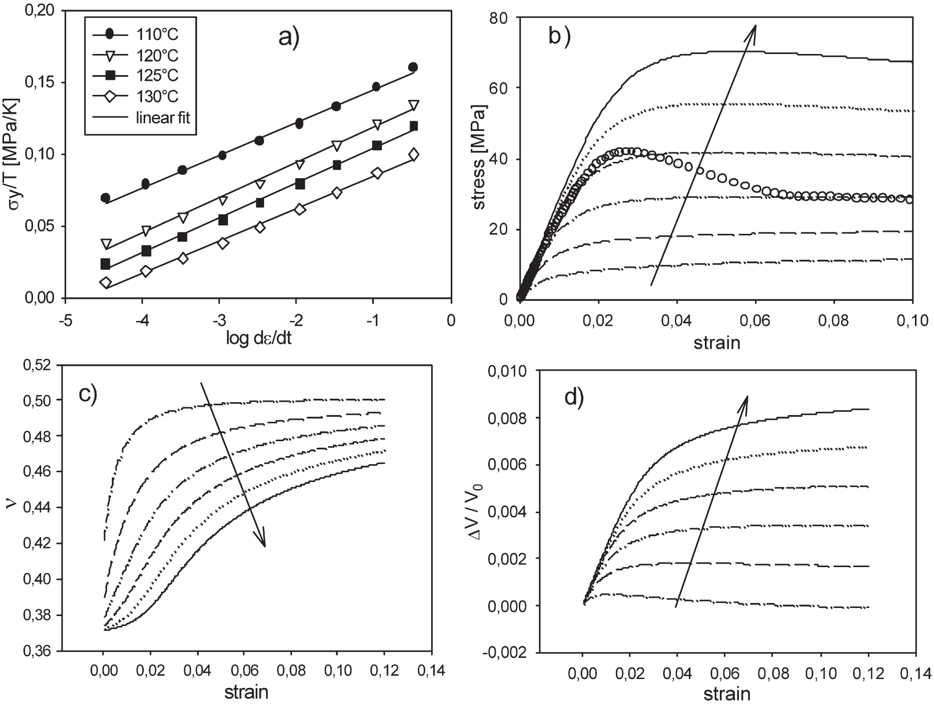

Figure 4.

a) The simulated results of the yield stress (symbols) of Polycarbonate at different temperatures as function of the deformation rate. The data are linearly fitted (lines) conforming to the Eyring type behaviour. b) The stress-strain behaviour as function of the strain rate at $T = 120\,^{\circ}$C and $t_e = 10^4$s. The symbols represent the experimental data obtained at a strain rate $\dot{\varepsilon} = 0.032\text{s}^{-1}(\log \dot{\varepsilon} \approx -1.5)$. Behind the yield point the corresponding simulated data deviate from the experimental ones as the numerical simulations account only for homogeneous deformations. c-d) The Poisson's ratio,ν, and the departure from the initial volume, $\Delta V/V_0$ vs. strain as function of the strain rates corresponding to the data of figure 4b. The arrows indicate increasing strain rates.

in bodies of finite size the volume recovery behaviour at a point becomes perturbed by the additional effect of the local isotropic part of the stress tensor originated by the external perturbations (mechanical or thermal). This aspect is geometrically described in terms of volume departure from equilibrium, δ, and fictive temperature, T_f, conforming with the KAHR and TNM variables, respectively. Thus our approach starts replacing the pressure with the spherical part of the stress tensor in the KAHR equation. This is a conceptual point (even if reached with minimal changes of the existing formalisms) since in this way a constitutive link has been established between the structural relaxation and the stress tensor. Then, the KAHR model is modified as follows:

$$\delta^f = \frac{v - v^f_\infty}{v^f_\infty} = \int_0^\xi \left(-\Delta\alpha \frac{dT}{d\xi'} - \frac{1}{3}\Delta k \frac{d\sigma}{d\xi'}\right) \times M(\xi - \xi')d\xi' \qquad (1)$$

where δ^f is the dimensionless volume with respect to the equilibrium fictive volume, v^f_∞ (defined below), T is the temperature, $\sigma = \sum_{i=1}^3 \sigma_{ii}$ the isotropic part of the stress tensor, $\Delta\alpha = \alpha_\infty - \alpha_0$ and $\Delta k = k_\infty - k_0$ with α_∞, k_∞ and α_0, k_0 being the thermal expansion and the isothermal

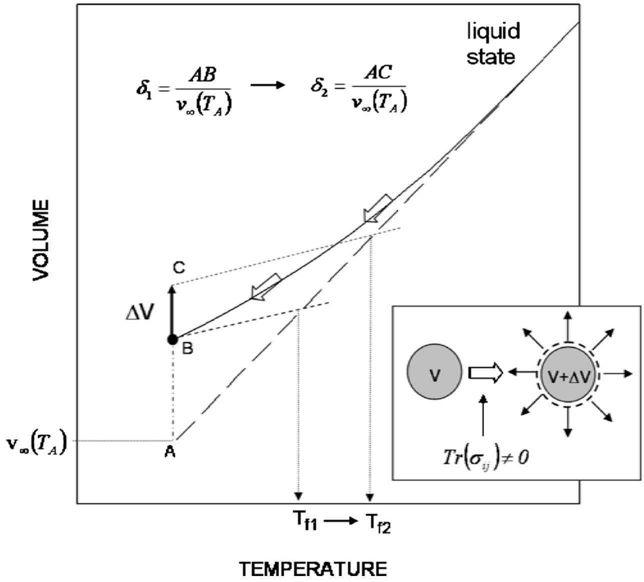

Figure 5.

Geometric description of the volumetric effects generated by the isotropic part of the stress tensor. The arrows indicate a specific thermal history at a given point within the sample that drives the point to the "state" B. The mechanical loading perturbs "locally" the volume by an amount ΔV and consequently alters its relaxation behaviour.

compressibility coefficients in the liquid, *l*, and in the glassy, *g*, state, respectively . ξ is the reduced time defined as follows:

$$\xi = \int_0^t \frac{dt'}{a_T a_\sigma a_\delta} \tag{2}$$

where a_T, a_σ, a_δ, are the shift factors describing the dependence of structural relaxation times on temperature, mechanical stress and structure, and

$$M(\xi) = \exp\left[-\left(\frac{\xi'}{\tau_r}\right)^\beta\right] \tag{3}$$

is the memory function expressed by the stretched exponential. β is the shape parameter and τ_r the characteristic relaxation time at a reference temperature.

In order to numerically solve Equation (1) one needs to couple it with a material constitutive equation establishing the relationships between stress and strain. We will use the formalism of the constitutive equation for linear viscoelastic material behaviour within the domain of reduced time (defined above):

$$\sigma_{ij} = \delta_{ij} \int_0^\xi \mathrm{B}(\xi - \xi') \frac{d}{d\xi'} (\varepsilon - \theta) d\xi + \int_0^\xi G(\xi - \xi') \frac{d}{d\xi'} \left(\varepsilon_{ij} - \frac{1}{3}\delta_{ij}\varepsilon\right) d\xi' \tag{4}$$

where B and G are the bulk the shear relaxation moduli, $\varepsilon = \sum_{i=1}^{3} \varepsilon_{ii}$ and θ is the free deformation due to the thermal effects.

Our approach generates a "stress clock" addition within the phenomenology of structural relaxation. The viscoelastic and structural phenomena are naturally linked through the principles of continuum mechanics, while the liner viscoelasticity and the KAHR equations written in the reduced time domain are the mathematical formalisms utilised in the numerical simulations. The "reduced time" contains the factors that alter the timescales of the volumetric as well as the viscoelastic responses. It is assumed that the logarithm of the relaxation time is a linear function of the spherical part of the stress tensor, the temperature and the structure (the dimensionless volume in the framework of the KAHR theory). The details of the numerical simulations are reported elsewhere and can be summarized as follows:

a) only two sets of experimental data are required (namely , the PVT and the linear shear relaxation modulus). In fact, the bulk relaxation modulus, B, is obtained through the ‘‘experimental’’ knowledge of the memory function;
b) the parameters of the KAHR theory are calculated on the basis of the PVT data and remain fixed once and for all;
c) the numerical simulations claim only for the loading and/or thermal histories as input data.

It was verified that the simulations succeed also under much more complex loading histories (the so called protocols II and III, not shown here)[6] with a quality of the results of the kind showed in Figures 2,3,4 and 6.

Discussion

After the above descriptions we are now ready to discuss the results in terms of yield and stress-strain behaviour. The simulation starts assuming a rapid quench from T_g+20 K down to T_g and holding the temperature constant. Then, the tests were numerically performed at constant rate of deformation, $\dot{\varepsilon}$, $(10^{-5} \leq \dot{\varepsilon} \leq 5s^{-1})$, different elapsed times t_e $(10^3 \leq t_e \leq 10^6 s)$, and different temperatures, T $(T_g - 32°C \leq T \leq T_g - 12°C)$. The results are reported in Figures 4a–d and in Figure 6. Figures 4a–d summarized the response at a given aging time (namely, 10^4s), while the responses at a fixed temperature are reported in Figure 6. For the sake of clarity, only part of results are illustrated with respect to the possible combinations generated by the parameters in play (namely, the temperature, the strain rate and the aging time). In Figure 4a the typical Eyring plot is reported. The data points in terms of yield stress at a given temperature come from the maxima exhibited by the stress-strain curves of the kind illustrated in Figure 4b, where, for instance, the simulations have been obtained at T = 120 °C. These two sets of results are commonly

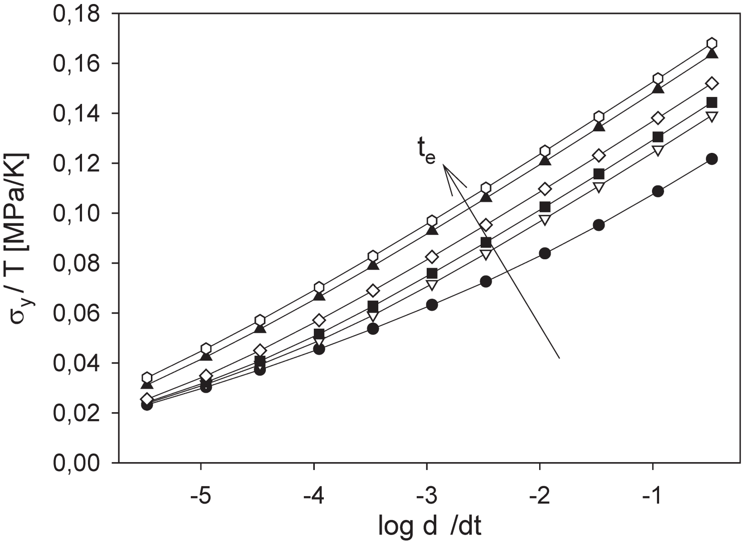

Figure 6.
Aging time dependence of the yield stress at 120 °C (lines: guide to eye).

reported in literature.[16–18] Our modelling approach correctly predicts that the yield stress (i.e. the maximum of the stress strain curve) increases at increasing strain rates and that it scales linearly with the logarithm of the strain rate at any temperature with a unique slope (see for comparison ref. 16). Despite the fact that we consider the above simulation extraordinarily sound, a real breakthrough in the interpretation of the stress-strain behaviour of amorphous polymers arises from a simultaneous view of Figures 4b and 4c,d. In fact, in Figure 4c and 4d a brand new kind of simulated results, corresponding to the stress-strain curves reported in Figure 4b, are shown in terms of volume departure from the unloaded state, $\Delta V/V_0$, and Poisson's ratio, ν, respectively, as function of the strain. In the range of strain tested, $\Delta V/V_0$ appears as a monotonic increasing function of the strain at higher strain rates, while it exhibits a non monotonic behaviour at lower strain rates. Indeed, at the lowest simulated strain rate, $\Delta V/V_0$ falls into negative values. It is quite surprising to see that one cannot find any correspondence between, say, the maxima in the stress-strain curves and the corresponding volumetric behaviour. For example, looking at the stress-strain curve obtained at the highest strain rate, yielding occurs at a strain value of about 4%, while, at that strain, $\Delta V/V_0$ doesn't show any abrupt change to be ascribed to a turning point. The same considerations can be done looking at the corresponding data in terms of Poisson's ratio, ν (Figure 5d). It is apparent that, at the strain corresponding to the yield stress, ν achieves a value that is far from being close to 0.5. Indeed, the saturation value (namely, $\nu = 0.5$) is not attained even at the highest simulated strain. It is worth mentioning that our simulations cannot account for the instability phenomena (i.e., necking) that occur just behind the yield point. So that only homogeneous deformations are of concern. To illustrate, in Figure 4b the experimental and the simulated data at $\dot{\varepsilon} = 0.032 s^{-1}$ ($\log \dot{\varepsilon} \approx -1.5$) are compared. The experimental stress-strain curve is almost fulfilled until the yield stress and the simulated and experimental yield stresses (i.e. the maxima in both stress-strain curves) almost coincide. The apparent discrepancies between the simulated and the experimental behaviour can be appreciate in what follows. In the experimental curve the yielding point appears "anticipated" at lower strain with respect to the simulations. This is not surprising since necking occurs (i.e. the stress drops) within localised zones where the actual (true) strain is higher than the nominal strain. It is also worth mentioning that the "intensity" of necking phenomena depends on the previous thermal histories and, in particular, freshly quenched amorphous polymers undergo homogeneous deformations, so that they do not exhibit necking so much as sharp maxima in the stress strain curves (indeed, these are the characteristics of the of the actual simulated behaviour). Anyway, even if we limit the discussion to the yield point, the substantial result is that the Eyring-type behaviour is fulfilled at least within the strain rate interval examined. In other words we can predict the yield stress in a quite reliable manner, while at the same time the background of the simulations gives a deep insight into the phenomenology in absence of instability phenomena (i.e. shear banding, necking, crazing an so on). For instance, we recall that the Eyring theory is based on the transition state of viscous liquids under shear flow, while it is apparent (by looking at the simultaneous evolutions of both the stress and the volume departure from the initial unloaded state) that, at the yield point, the glass is far from being a liquid.

Some adjunctive knowledge of the stress strain behaviour of glassy materials can achieved by looking at Figure 6, where the yield stress is reported at different "aging times", t_e, ($10^3 \leq t_e \leq 10^6 s$) as function of the strain rate, at T = 120 °C. The dramatic role of the aging time can be rapidly appreciate by comparing the simulated data of Figure 6 and Figure 4a: in the range of aging times investigated the yield stress variations are of the same magnitude of those observed in the temperature interval 110–130 °C.

Conclusions

The volumetric as well as the viscoelastic responses of mechanically stimulated glasses have been reviewed. It has been shown that constitutively coupling the structural and the viscoelastic relaxation phenomena both the substantial and the subtle features appeared in literature along the last three decades can be reliably simulated. The numerical simulations make use of only two simple data sets (namely, the PVT and the linear shear relaxation modulus. The model parameters derive directly from the two sets of experimental data and remain fixed once and for all. This allows us to affirm that the volumetric and the viscoelastic responses in the glassy state are already "written" into PVT and viscoelastic (equilibrium) data in a way that *"the phenomenology of mechanically stimulated glasses can only be studied in the framework of a theory connecting the volumetric as well as the viscoelastic phenomena, since their mutual interaction*". With the present theory the substantial and the subtle features of mechanically stimulated glasses (namely, the shift rate contraction with the stress, the invariance of the volume recovery baseline and the Eyring-type behaviour of glassy polymers) can simultaneously predicted, a case never presented before.

[1] L. C. E. Struik, "*Physical Aging in Amorphous Polymers and Other Materials*" Elsevier, Amsterdam **1978**.

[2] G. B. McKenna, *J. Phys.: Condens. Matter* **2003**, *15*, S737.

[3] A. J. Kovacs, J. J. Aklonis, J. M. Hutchinson and A. R. Ramos, *J. Polym. Sci., Polym. Phys. Ed.* **1979**, *17*, 1097; A. R. Ramos et al., *J. Polym. Sci., Part B: Polym. Phys.* **1988**, *26*, 501.

[4] A. Q. Tool, *J. Am. Ceram. Soc.* **1946**, *29*, 240; O. S. Narayanaswamy, *J. Am. Ceram. Soc.* **1971**, *54*, 491; M. A. DeBolt, A. J. Easteal, P. B. Macedo, and C. T. Moynihan, *J. Am. Ceram. Soc.* **1976**, *59*, 16.

[5] G. Adam and J. H. Gibbs, *J. Chem. Phys.* **1965**, *28*, 139.

[6] L. Grassia, A. D'Amore, *Physical Review E* **2006**, *74*, 021504.

[7] L. C. E. Struik, *Polymer* **1997**, *38*, 4053.

[8] L. Grassia and A. D'Amore, *Macromol. Symp.* **2005**, *228*, 1.

[9] G. Astarita, *J. Rheol.* **1990**, *34*, 275.

[10] H. A. Barnes, *J. Non-Newtonian Fluid Mech.* **1999**, *81*, 133.

[11] I. Emri and W. G. Knauss, *Polym. Eng. Sci.* **1987**, *27*, 86.

[12] S. R. Lustig, R. M. Shay Jr., and J. M. Caruthers, *J. Rheol.* **1996**, *40*, 69.

[13] 38 J. M. Caruthers, D. B. Adolf, R. S. Chambers, and P. Shrikhande, *Polymer* **2004**, *45*, 4577.

[14] D. B. Adolf, R. S. Chambers, and J. M. Caruthers, *Polymer* **2004**, *45*, 4599

[15] A. Tobolsky, and H. Eyring., *J Chem Phys* **1943**, *11*, 125

[16] 1972 C. Bauwens-Crowet et al. *J. of Materials Science* **1972**, *7*, 176.

[17] J. M. Hutchinson, S. Smith, B. Horne, and G. M. Gourlay, *Macromolecules* **1999**, *32*, 5046.

[18] I. M. Ward "*Mechanical Properties of Solid Polymers*", John Wiley & Sons, **1983**.